

Effect of Mushy State Rolling on the Microstructure, Microhardness, and Microtexture in Al-4.5wt.%Cu-5wt.%TiB₂ In Situ Composite

MONALISA MANDAL^{1,2} and RAHUL MITRA¹

1.—Department of Metallurgical and Materials Engineering, Indian Institute of Technology Kharagpur, Kharagpur, West Bengal 721302, India. 2.—e-mail: monalisa0212@gmail.com

Al-4.5wt.%Cu-5wt.%TiB₂ in situ composite, fabricated by stir casting through a mixed salt reaction route process, needs further processing to exclude casting defects. Mushy state rolling has been developed as an easy and energy-efficient method for microstructural refinement and improvement in mechanical properties. It has been carried out at 621°C and 632°C with 20 vol.% and 30 vol.% of liquid, respectively, for up to 5% reduction in thickness. Mushy state rolling of the as-cast composite gives rise to a bimodal microstructure, which consists of very fine equiaxed grains adjacent to the rolled surface and comparatively larger elongated grains away from the rolled surface of the sample. Microhardness of the mushy state rolled sample has been observed to decrease gradually from edge to center of the rolled sample. The presence of the dislocation tangles and subgrains formed by dynamic recovery within solid-state deformed elongated grains and formation of recrystallized grains just adjacent to the second-phase particles have been examined with the help of electron backscattered diffraction and transmission electron microscopy analysis.

INTRODUCTION

Recently, metal matrix composites (MMCs) have been developed due to their potential for use as lightweight structural materials in the automotive and aerospace industries.¹ MMCs contain rigid and high-strength ceramic reinforcements embedded within the ductile metal or alloy matrix. The MMCs are of interest as these materials can be designed to have a desirable combination of strength, ductility, and toughness on the basis of the individual properties of each constituent phase. The Al alloys are considered to be favored as matrix materials because of their high strength-to-weight ratio, high stiffness, age-hardenability, superior corrosion resistance, low thermal expansion coefficient, and high damping capacity.^{1–3} In particular, the discontinuously reinforced Al-based composites (DRAs) are preferred to continuous fiber-reinforced composites to retain the isotropy of the material properties. The ceramic reinforcements can be used as filler material in MMCs. Generally, Al-based composites reinforced with ceramic particles like SiC, TiB₂,

Al₂O₃, and B₄C have become very popular choices for structural applications as their presence does not change the density of the matrix much, but it improves the strength and modulus of the composites.^{4–9} Among the above-mentioned ceramic reinforcements, TiB₂ has been chosen as the reinforcement in this study for its high hardness (3rd hardest ceramic material available, 86 HRA or 960 HV), high elastic modulus (530 × 10³ GPa), high melting point (2790°C), sound thermal stability, and no reactivity with the molten Al during production through a salt–metal reaction.^{3,10} DRAs have been reported to show the best properties if fabricated via in situ route. In situ DRA composites have particles of fine size (micron or submicron) with almost uniform distribution and much cleaner matrix-reinforcement interfaces.¹¹

The synthesis of DRAs is well developed, and different techniques are well documented.² Secondary processing of the cast composites is needed not only to eliminate casting defects but also to tailor microstructures for obtaining desirable mechanical properties. A thorough investigation and optimization of mushy

state rolling (semisolid processing) of cast Al-4.5wt.%Cu-5wt.%TiB₂ composite has been reported.¹² Studies on mechanical properties including hardness and tensile properties,^{12,13} wear behavior,^{5,8} and aging effects¹³ carried out on the mushy state rolled, in situ Al-4.5wt.%Cu-5wt.%TiB₂ composites, have shown significant improvement over those of its as-cast samples. It has been reported earlier that the flow stress required for plastic deformation is dependent on the amount of liquid content present in the mushy state.^{14,15} Electron backscattered diffraction investigation (EBSD) has been scarcely carried out¹⁶ on DRAs, and there is no earlier report on the EBSD analysis of the mushy state rolled, in situ Al-4.5wt.%Cu-5wt.%TiB₂ composite.

The present article shows the effect of mushy state rolling on the evolution of microstructure, microhardness, and microtexture of Al-4.5wt.%Cu-5wt.%TiB₂ in situ composite. In the present work, EBSD has been used to characterize the recrystallized grains nucleated by the particle stimulation, as well as the dislocation substructure formed due to recovery.

EXPERIMENTAL DETAILS

An Al-4.5wt.%Cu alloy matrix was prepared by melting of an appropriate amount of commercially pure grade Al and Al-33wt.%Cu master alloy. Furthermore, a salt mixture of K₂TiF₆ and KBF₄ was added in the stoichiometric ratio into the melt at 800°C, held for 1 h, and then stirred for every 10-min interval, to form the TiB₂ particles in situ.¹² The as-cast samples were subjected to mushy state rolling at 621°C and 632°C for having 20 vol.% and 30 vol.% liquid, respectively, at the time of deformation. The samples were subjected to 3% to 4% reduction in thickness. Reduction in thickness was limited to 5% because of alligating, occurring on higher reduction per pass.¹² The samples mushy state rolled with 20 vol.% and 30 vol.% liquid have been labeled as 20l4r_MRC and 30l3r_MRC, respectively. To prevent the heat loss during transferring of the sample from furnace to the rolling mill, the portable furnace for reheating of the as-cast composite samples to mushy zone temperature was placed very near the rolling mill. After mushy state rolling, the L-T surfaces of the composites as shown in Fig. 1a, were characterized. Figure 1b shows schematically the edge and center sections of a typical L-T surface. The mushy state rolled samples were tested with a Vickers microhardness tester operated at 100-gf load. Scanning electron microscopy (SEM) and phase identification with the help of the x-ray diffraction (XRD) technique and EBSD were carried out. EBSD scans were carried out to analyze the recrystallized grains, subgrains, and dislocation tangle map. The samples were examined in a transmission electron microscope (TEM) to

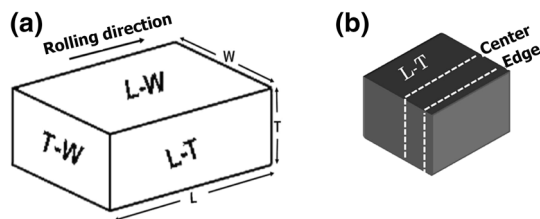


Fig. 1. Schematic illustration of mushy state rolled samples: (a) showing different planes in (b) edge and middle section of the L-T plane.

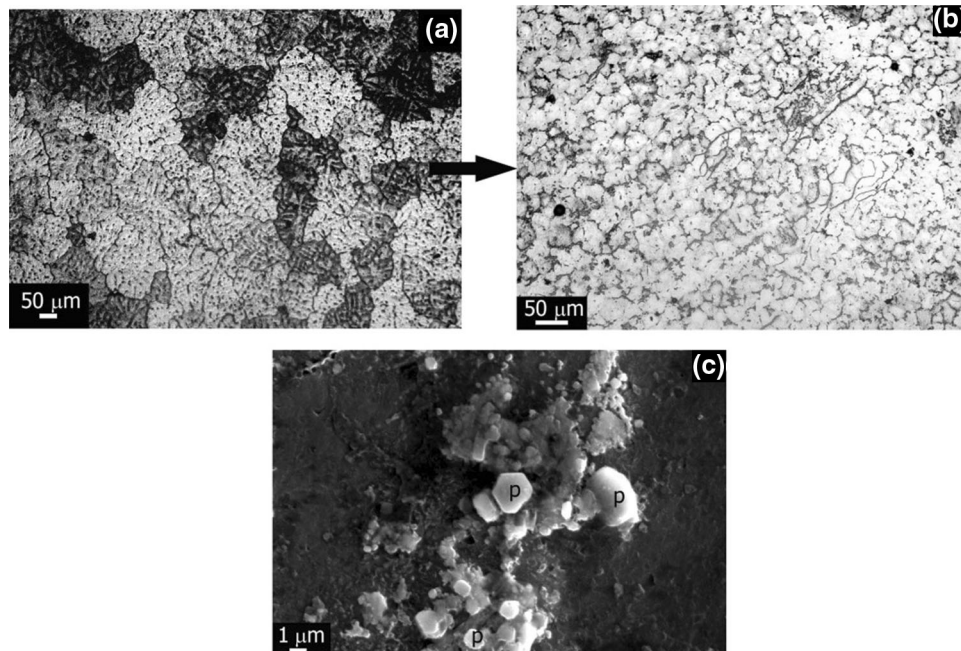


Fig. 2. Optical micrographs of (a) as-cast Al-4.5wt.%Cu alloy having dendritic structure; (b) as-cast Al-4.5wt.%Cu-5wt.%TiB₂ in-situ composite depicting rosette-type grain structure; and (c) SEM image of as-cast Al-4.5wt.%Cu-5wt.%TiB₂ in situ composite. TiB₂ particles are shown as P.

observe the dislocation substructure and freshly recrystallized grains adjacent to the second phase precipitates and particles.

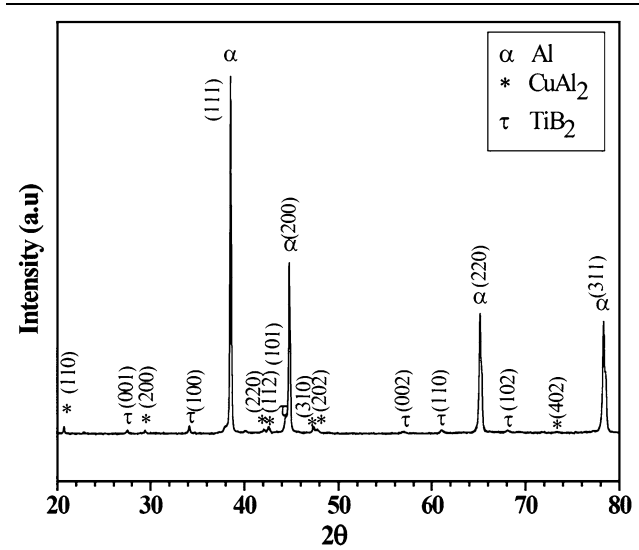


Fig. 3. XRD phase analysis of as-cast Al-4.5wt.%Cu-5wt.%TiB₂ in situ composite.

RESULTS AND DISCUSSION

Microstructure and Phase Studies

Figure 2a and b shows the optical micrographs of the as-cast base alloy and in situ composite, respectively. The presence of in situ formed TiB₂ particles completely transforms the dendritic microstructure of the alloy into a rosette-type grain structure. Figure 2c shows the SEM micrograph of the TiB₂ particles sitting at the grain boundaries of the as-cast in situ composite. The TiB₂ particles are generally hexagonal in shape and have sizes in the range of 0.2 μm to 1.5 μm. The phase identification has been confirmed with the help of XRD analysis (Fig. 3). Mushy state rolling of the as-cast composite has transformed the rosette-shaped microstructure into that with globular grains having a size gradient (measured by ImageJ software on SEM images) from edge to center. Figure 4a–d shows the optical micrographs depicting the grain structure of either the edge section or the center section of 2014r_MRC or 3013r_MRC. For both rolling conditions, the edge section has a bimodal distribution of small and large grains of almost equiaxed shape. The average sizes of fine and large grains in bimodal distribution are estimated as ~10 μm and ~45 μm, respectively. The second-phase precipitates and particles are homogeneously distributed along the grain

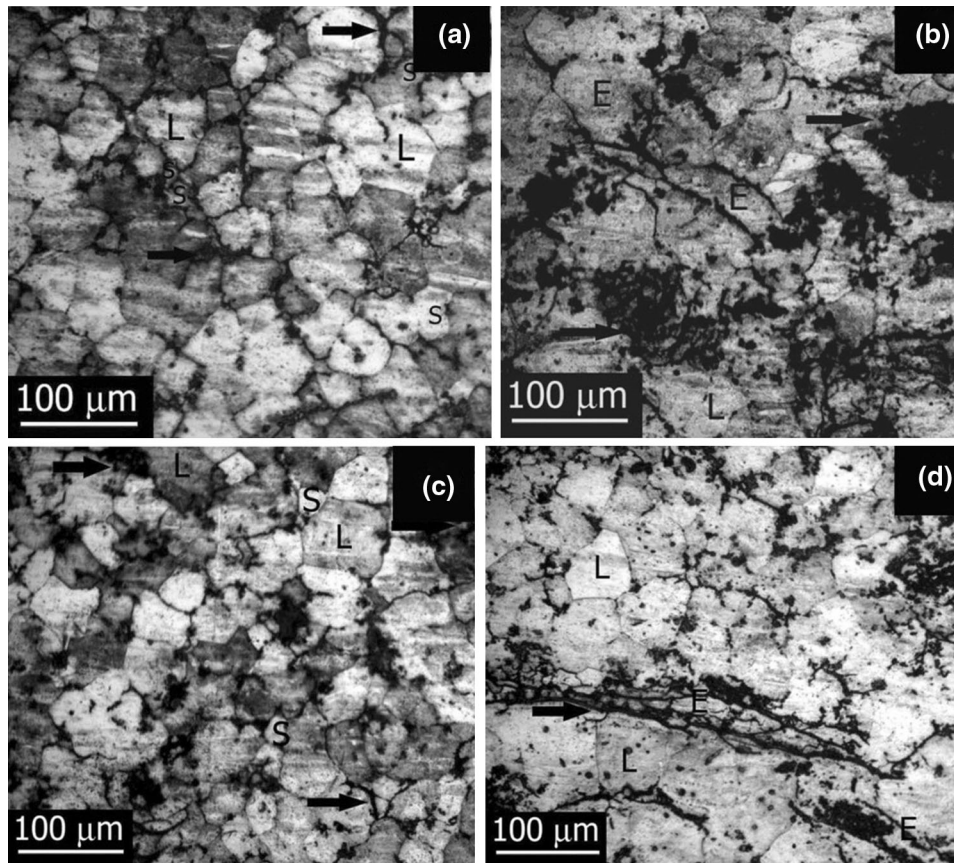


Fig. 4. Optical micrographs of mushy state rolled composites. Particles are shown with black arrows. L, S, and E are, respectively, denoting large, small, and elongated grains: (a) 2014r_{edge}, (b) 2014r_{center}, (c) 3013r_{edge}, and (d) 3013r_{center}.

boundaries of the edge section's grains. The second-phase precipitates and particles pin down the grain boundaries and help in the evolution of equiaxed

grains. On the contrary, the grains at the center are comparatively large and elongated in shape, and the clusters of second-phase precipitates and particles have been observed irregularly distributed along the grain boundaries, as well as within the grains. Such irregular distribution of particles can be attributed to the accelerated growth of some grains, whose boundaries have not been restricted by the Zener pinning mechanism. During mushy state rolling, the liquid present within the workpiece comes in contact with the rolls, which were kept at the ambient temperature, and introduces a temperature gradient. This temperature gradient has aided the rapid solidification of the liquid and has resulted into fine equiaxed grains at the edge section. At the center, most of the grains are deformed in solid state and thus appear to be elongated in shape.

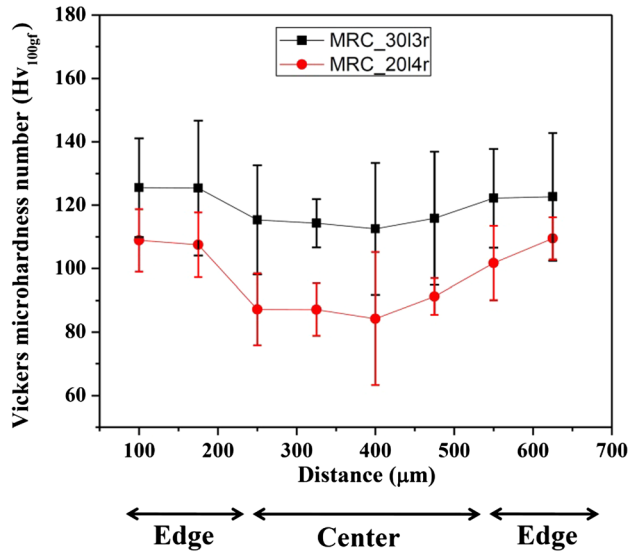


Fig. 5. Vickers microhardness plot of MRC_30I3r and MRC_20I4r on the L-T surface from edge to edge.

Microhardness Studies

Figure 5 presents the plots of Vickers microhardness variation from edge to edge on the L-T surface of the mushy state rolled samples. The microhardness decreases gradually from edge to center, as shown in this figure. The indentations have been intentionally made on the Al alloy matrix. A high

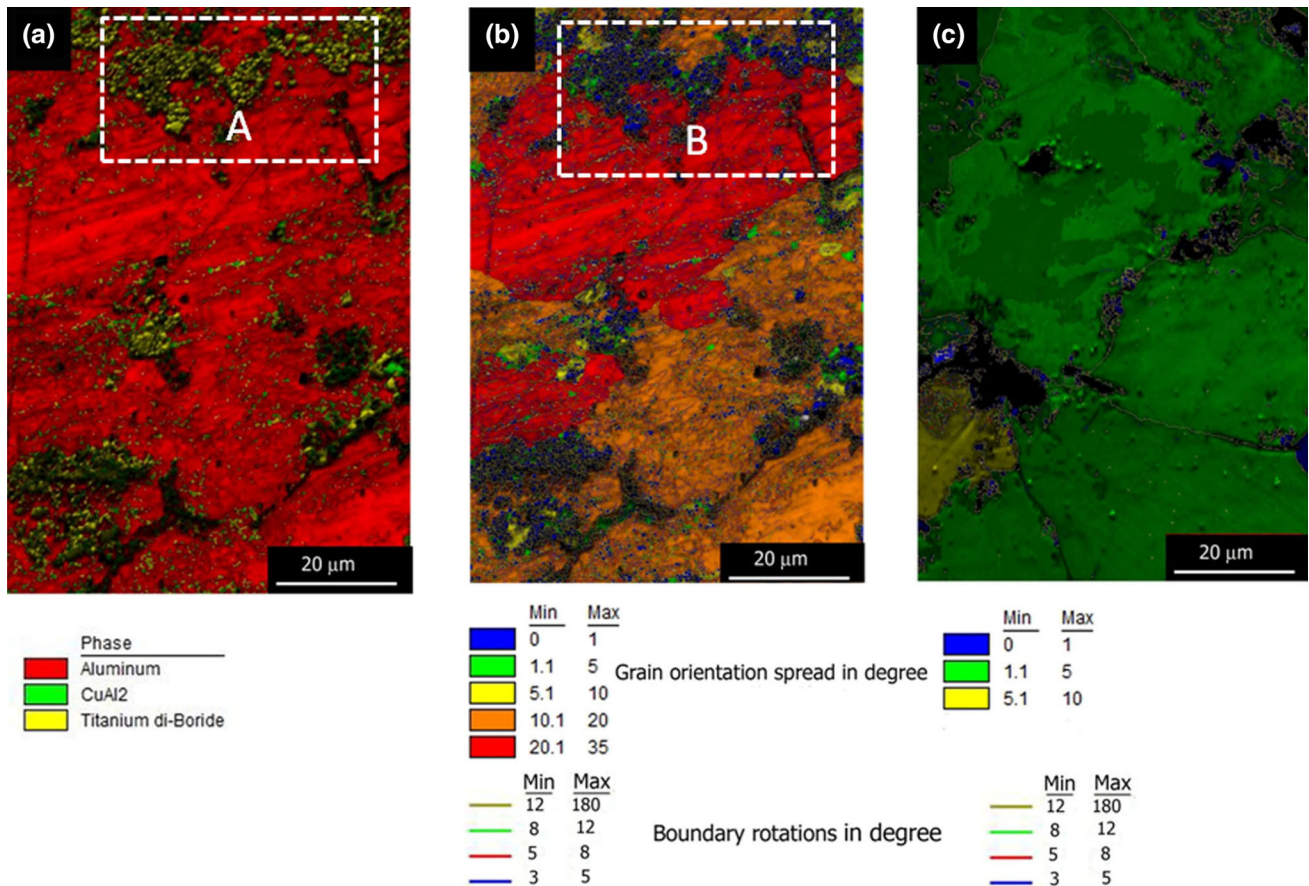


Fig. 6. EBSD maps of 20I4r_MRC on the L-T surface: (a) phase map and phase index at the center; (b) grain orientation spread map with boundary and orientation spread index at the center; and (c) grain orientation spread map with boundary and orientation spread index at the edge. Regions of interest are marked as A and B in (a) and (b), respectively.

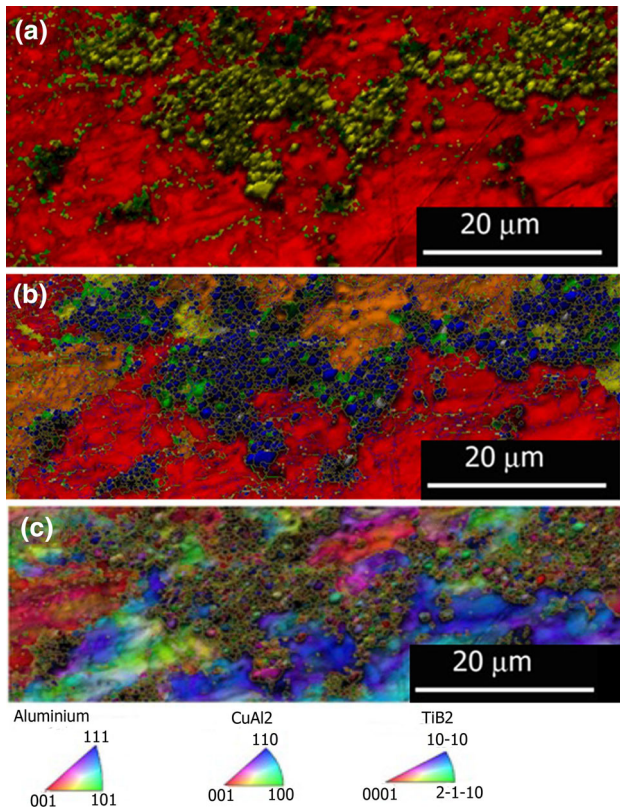


Fig. 7. Enlarged view of the EBSD maps of 2014r_MRC on the L-T surface at the center: Magnified views of the regions (a) marked as “A” in phase map of Fig. 6a, (b) marked as “B” in grain orientation spread (GOS) map of Fig. 6b, and (c) the same region marked as “B” in Fig. 6b of inverse pole figure (IPF) map.

hardness value at the edge can be attributed to a larger volume fraction of finer equiaxed grains, whereas a lower hardness value recorded at the center could be due to the large volume fraction of coarse grains at this location. For the higher liquid fraction, 3013r_MRC has shown a high hardness value in comparison with 2014r_MRC. For 30 vol.% liquid, the temperature gradient between the sample and the roll surface is higher compared with that in the case of the 2014r_MRC. Both samples have been subjected to almost similar reduction in thickness, and it is assumed that as the deformation is very less, it does not have much effect on the difference in the hardness value. The comparable difference in the hardness values has mainly come from grain boundary hardening.

Microtexture Analysis

EBSD scans of both samples have been carried out on the L-T surfaces. For comparative studies, all scans have been performed on an equal area ($55 \times 85 \text{ m}^2$) with $0.2 \mu\text{m}$ step size. During data acquisition and postprocessing, all input variable parameters have been kept identical. Figure 6a and b shows respectively the phase-map and grain

orientation spread (GOS) map of the center of the 2014r_MRC sample. Figure 6c shows the GOS map of the edge of the 2014r_MRC sample. Figure 7a–c shows the enlarged view of the phase map, GOS map, and inverse pole figure (IPF) map of the center of the 2014r sample: Fig. 6a–c, respectively. The TiB_2 and CuAl_2 particles are observed along with the Al-Cu solid solution phase as shown in Fig. 7a. The GOS map provides the results of grain-based local misorientation analysis. It shows the deviation of the orientation of each pixel within a grain from the average orientation of that grain. Figure 6b and c gives the orientation spread within grains, which are completely enclosed by high-angle grain boundary criteria (boundary rotation: 12° to 180°) of the center and edge of the 2014r_MRC sample, respectively. The maximum spread within a grain has been observed as 32.5° and 9° , respectively, in the center and edge of the 2014r_MRC sample. Grains with less than equal to 1° GOS values have also been observed at both the center and the edge of the 2014r_MRC sample. The enlarged view of the GOS map of the center shows grains with less than equal to 1° orientation spread nucleated just adjacent to the second-phase particles. These fine grains are completely enclosed within high-angle boundaries, and almost no low-angle boundaries are found inside that. Figure 7c has confirmed that these are grains having different orientations with respect to each other. These grains have probably formed due to dynamic recrystallization of unmelted Al during mushy state rolling. The grains with high GOS values have been observed to have various low-angle boundaries inside. It has been assumed that these low-angle boundaries are a consequence of the dislocation tangle structure. Dynamic recovery is common in Al because of its high stacking fault energy.

TEM has been carried out to confirm the formation of dislocation tangles and subgrains within large Al grains during deformation. Figure 8a shows the bright field TEM image of dislocation tangles within a large Al grain. Figure 8b shows the TEM image of a TiB_2 particle inside the Al matrix. Figure 8c shows the TEM image of an area adjacent to second-phase particles and its selected area electron diffraction pattern (SAEDP). The SAEDP is a ring pattern of Al, which can be attributed to the formation of randomly oriented fine grains, which are preferentially located just adjacent to second-phase particles. The strain field around the particles (size range $0.2 \mu\text{m}$ to $1.5 \mu\text{m}$) has aided the nucleation of new strain free grains confirming the occurrence of dynamic recrystallization.^{17,18} Therefore, it can be inferred that particle-stimulated nucleation and dynamic recrystallization might have been taken place due to mushy state rolling. Dynamic recovery during mushy state rolling has led to the formation of subgrains and a dislocation network within large grains. A similar microtexture has been observed at the edge section of the 2014r-

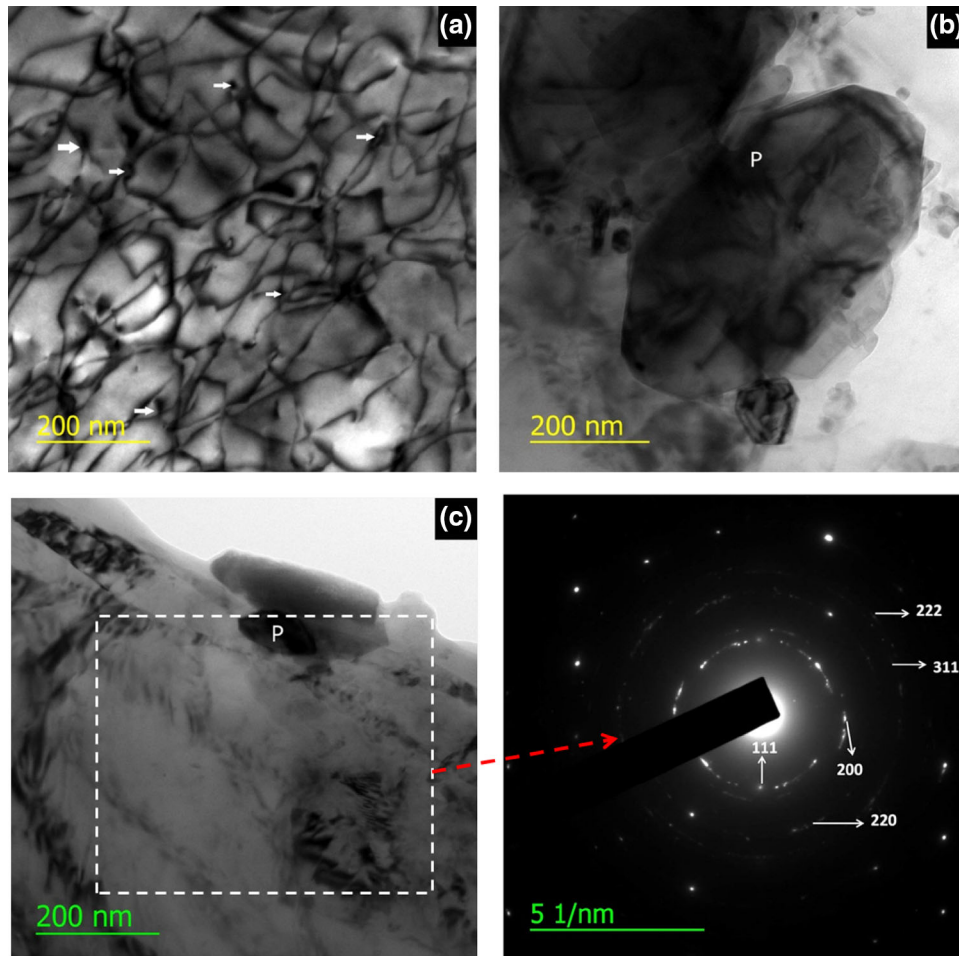


Fig. 8. TEM images of the 2014r_MRC sample at the center of L-T surface. (a) Bright field image within a large grain showing dislocation networks. Particles rendering dislocation are shown with arrows (b) TiB₂ particle (~0.6 μm). (c) Bright field image of an area adjacent to a TiB₂ particle (P) and SADP of the dotted area; the ring pattern of Al has confirmed the presence of fine recrystallized grains.

MRC sample with relatively less orientation spread within a large grain (Fig. 6c), which is suggestive of dynamic recovery during deformation.

CONCLUSION

The following conclusions can be drawn from the present study. The mushy state rolling transforms the rosette-shaped microstructure of the as-cast in situ composite into a gradient microstructure. The gradient grain size distribution leads to an increase in microhardness from center to edge of the mushy state rolled composite with different liquid fractions. Particle-stimulated nucleation has been confirmed by the presence of recrystallized grains near the second-phase particles in EBSD and TEM studies. Dynamic recrystallization appears to have taken place only near particles at the time of mushy state rolling. A high GOS value within large Al grain and the presence of low-angle boundaries have been observed through EBSD studies, whereas formation of dislocation tangles has been confirmed

by the TEM studies. Such evidence of dynamic recovery is found in the grains subjected to solid-state deformation during mushy state rolling.

REFERENCES

1. S. Rawal, *JOM* 53, 14 (2001).
2. B.S.B. Reddy, K. Das, and S. Das, *J. Mater. Sci.* 42, 9366 (2007).
3. S. Suresh, N. Shenbag, and V. Moorthi, *Proc. Eng.* 38, 89 (2012).
4. S.C. Tjong and K.C. Lau, *Mater. Sci. Technol.* 16, 99 (2000).
5. I.G. Siddhalingeswar, D. Deepthi, M. Chakraborty, and R. Mitra, *Wear* 271, 748 (2011).
6. A.V. Smith and D.D.L. Chung, *J. Mater. Sci.* 31, 5961 (1996).
7. S.C. Tjong, S.Q. Wu, and H.G. Zhu, *Compos. Sci. Technol.* 59, 1341 (1999).
8. M.A. Herbert, C. Sarkar, R. Mitra, and M. Chakraborty, *Wear* 265, 1606 (2008).
9. R. Ipek, *J. Mater. Process. Technol.* 162, 71 (2005).
10. R.G. Munro, *J. Res. Natl. Inst. Stand. Technol.* 105, 709 (2000).
11. R. Mitra, W.A. Chiou, M.E. Fine, and J.R. Weertman, *J. Mater. Res.* 8, 2380 (1993).
12. M.A. Herbert, C. Sarkar, R. Mitra, and M. Chakraborty, *Metall. Mater. Trans. A* 38, 2110 (2007).

13. I.G. Siddhalingeswar, M. Chakraborty, M. Herbert, and R. Mitra, *Mater. Sci. Eng. A* 528, 1787 (2011).
14. M.C. Flemings, *Solidification Processing* (New York: McGraw-Hill Book Co., 1974), pp. 22–23.
15. M. Kiuchi and R. Kopp, *J. Jpn. Soc. Technol. Plastic.* 20, 826 (1979).
16. J. Corrochano, P. Hidalgo, M. Leblisch, and J. Ibáñez, *Mater. Char.* 61, 1294 (2010).
17. D.J. Jensen, N. Hansen, and F.J. Humphreys, *Acta Metall.* 33, 2155 (1985).
18. N. Hansen and B. Bay, *Acta Metall.* 29, 65 (1981).